AIAA Atmospheric and Space Environments Conference
2 - 5 August 2010, Toronto, Ontario Canada

AIAA 2010-7983

Computational Prediction of Propeller Performance in Icing Conditions

Greg Busch[1] and Michael Bragg[2]
University of Illinois at Urbana-Champaign, Urbana, IL 61801

The objective of this investigation was to develop a computational methodology to quantify propeller performance in icing conditions and to identify areas where additional research is required. Propeller blade-section ice geometry was predicted using the ice accretion code LEWICE, the corresponding degradation in blade-section aerodynamic performance was predicted using the RANS code Fluent, and the blade-section performance was correlated to propeller performance with a blade-element code utilizing vortex theory. The results of this process were compared to experimental data obtained during a full-scale propeller icing test conducted at McKinley Climatic Laboratory at Eglin AFB. Ice shedding was found to be significant during these tests, and LEWICE was only able to accurately predict blade-section ice geometries by accounting for this shedding using experimental observations. Fluent predictions of blade-section aerodynamic performance were compared with experimental measurements obtained with artificial ice shapes in an earlier part of this investigation; agreement ranged from poor to good, depending on the blade section and ice geometry. The resulting predictions in clean and iced propeller performance were within 10% of the experimentally-measured values for two of the three icing conditions presented, and within 17% for the third set of conditions. This study has identified areas where research is needed to improve the accuracy of the predictions.

Nomenclature

α	angle of attack
α_i	induced angle of attack
b	airfoil model span
β	blade pitch angle
B	number of propeller blades
c	airfoil chord length
C_d	drag coefficient
$C_{d,min}$	minimum drag coefficient
C_l	lift coefficient
$C_{l,max}$	maximum lift coefficient
C_P	propeller power coefficient
C_T	propeller thrust coefficient
D	propeller diameter
dC_P	incremental power coefficient at a single blade section
dC_T	incremental thrust coefficient at a single blade section
η	propeller efficiency
J	propeller advance ratio
k	ice feature height
LWC	liquid water content
M	freestream Mach number
MVD	median volume diameter of water drops
OAT	outside air temperature
Re	freestream Reynolds number, based on the airfoil chord length
r	coordinate in the propeller radial direction
R	propeller radius

[1] Graduate Research Assistant, Department of Aerospace Engineering, currently at Air Force Research Laboratory, Space Vehicles Directorate, Member AIAA
[2] Professor of Aerospace Engineering, Executive Associate Dean for Academic Affairs, Fellow AIAA.

σ	blade solidity, $Bc/(\pi R)$
s	airfoil model coordinate along the surface length
SLD	super-cooled large droplet
w	induced velocity at propeller blade section
V_E	resultant velocity seen by propeller blade section
x	non-dimensional radial station, r/R
z	coordinate in the airfoil model spanwise direction

Introduction

Degradation of propeller performance in icing conditions may present a serious hazard to passenger safety, as ice accretion may cause considerable decreases in propeller thrust and efficiency. Recent icing flight tests have shown significant reductions in airspeed due to propeller blade ice accretion,[1] prompting the FAA to seek new methods for predicting the effects of ice on propeller performance. The objective of the current study was to develop a computational methodology with which the effects of ice accretion on propeller performance can be quantified.

The current study was the third phase of an FAA investigation to better understand the effects of ice accretion on propeller performance. The first phase was an experimental icing test conducted at McKinley Climatic Laboratory at Eglin Air Force Base on a full-scale propeller; this phase is discussed in detail by Dumont et al.[2] The second phase used ice accretion documentation obtained during the icing test (e.g., ice tracings, photographs, and video) to determine propeller blade-section aerodynamic performance degradation in icing conditions using artificial ice shapes. The iced blade-section performance was then related to the iced-propeller performance using a blade-element code; this work is discussed by Busch, Bragg, and Broeren.[3] In the third phase (the current study), the blade-section ice geometry, corresponding blade-section aerodynamic performance penalty, and resulting propeller performance degradation was predicted using computational tools. Each of these phases will be discussed in more detail later in this Introduction.

Several studies have already been conducted, both experimental and computational, to better understand the effects of ice on propeller performance. For example, Corson and Maynard[4] measured propeller performance on a full-scale propeller in the NASA Langley 16-ft. high-speed tunnel using artificial ice shapes. The shapes caused decreases in propeller efficiency of up to 3%. Preston and Blackman[5] conducted flight tests in natural icing conditions and documented efficiency losses of up to 19%. Neel and Bright[6] conducted additional flight tests and measured similar reductions in efficiency. To complement these tests, they developed a propeller analysis code using blade-element theory; this code predicted performance penalties similar to those observed during the flight tests. Neither of these latter studies thoroughly documented the ice accreted during the flight tests.

More recently, Korkan et al.[7] developed a theoretical model for analyzing propeller performance and were able to obtain good agreement with published experimental data. Another analytical model, an enhanced strip method, was developed by Miller et al.[8] This code used Bragg's 2-D droplet trajectory code[9] to calculate the accumulation parameter and collection efficiency, and empirical correlations of Gray,[10] Bragg,[9] and Flemming[11] to determine the effect of ice accretion on blade section performance. Since the Bragg and Gray correlations dealt only with C_d, a reduction in lift of 5% was assumed (relative to the clean value). It was found that analytical predictions of propeller performance agreed with the experimental measurements by Neel and Bright[6] to within the uncertainty of the correlations. It was also found that the output of the code depended substantially on the correlation used.

Reichhold et al.[12] used blade-element theory to explain how droplet impingement efficiencies greater than one could occur for propellers. Farag and Bragg[13] developed a three-dimensional droplet impingement code to determine the magnitude of three-dimensional effects on droplet trajectories in the vicinity of a propeller. The authors found that the number of propeller blades did not have a large effect on impingement characteristics, but the propeller power setting and nacelle/spinner geometry had a substantial effect. The code was again validated using three-dimensional experimental data and two-dimensional computational data which had been corrected for three-dimensional effects, and best agreement occurred when the spinner/nacelle was non-existent or very small. These studies show that two-dimensional strip methods can provide accurate results, although they may be affected by spinner/nacelle effects.

The studies described above suggest that propeller icing effects may be significant and the possibility that currently available computational tools may be used to predict propeller performance in icing conditions. Therefore, the FAA conducted an experimental icing test[2] to document propeller ice accretion and the associated reduction in thrust to better quantify icing effects and to provide a set of validation data. The test was conducted at the McKinley Climatic Laboratory at Eglin AFB on a full-scale, 8-ft. diameter propeller. Ice accretions were documented using

stop-action video during the test and with tracings after the test. Three tracings were taken along the propeller blade, at the mid-boot, 50%, and 75% radial stations. Still photographs were taken at the end of each test run for each accretion. The reduction in propeller thrust was also documented by taking measurements of thrust before and after the application of the icing cloud. Reductions in thrust averaged 5.9% and 13.4% for Appendix C and SLD conditions, respectively. The maximum measured thrust reduction was 21.2% in SLD conditions.

A second phase to this Eglin AFB investigation was conducted at the University of Illinois to provide additional validation data and to further evaluate the ability of a blade element code to relate blade section performance to propeller performance. Ice tracings obtained at three radial stations (the mid-boot, 50%, and 75%-stations) and photographs from the Eglin AFB icing test were used to construct artificial ice shapes for testing in a dry-air wind tunnel, based on techniques developed during the NASA Simulation Program.[14,15] Three two-dimensional airfoil sections were fabricated, representative of the mid-boot, 50%, and 75% propeller-blade stations. It was at these stations where the ice shapes were best documented during the icing test. The aerodynamic performance of these airfoils was measured in the clean condition and with artificial ice shapes representative of three runs conducted during the Eglin AFB icing test. The 33%-thick mid-boot blade section was found to be extremely sensitive to ice accretion, and extremely large decreases in lift and increases in drag were observed simply by tripping the boundary layer at 10% on the upper and lower surfaces. The 50% blade section exhibited more typical performance degradation due to ice, with decreases in $C_{l,max}$ ranging from about 13% (ice roughness after a low LWC encounter in App. C conditions) to 50% (in SLD conditions). The 6%-thick 75%-station blade section exhibited the smallest sensitivity of C_l to ice accretion, with a maximum decrease in $C_{l,max}$ of 26%. These performance data were analyzed in a blade-element propeller code to relate the blade-section aerodynamic performance degradation to overall propeller performance degradation, and comparisons with thrust data taken during the Eglin AFB icing test were made. Predicted reductions in C_T for the three cases analyzed were 11%, 8%, and 25%, compared with measured reductions of 6%, 9%, and 22%, respectively. To help determine potential causes of the differences between the predicted and measured results, several trade studies were conducted. It was found that using data from only three blade sections to represent the entire propeller blade had a notable effect on predicted propeller performance, and that uncertainties in ice geometry (and therefore blade section aerodynamic performance), such as those due to ice shedding, can be significant.

The overall objective of the FAA investigation was to develop a computational methodology to analyze propeller performance in icing conditions. However, the first and second phases used experimental techniques to determine iced propeller performance and blade-section aerodynamic performance, respectively. The current study was the third phase of the FAA investigation, and the objective of this phase was to use only computational tools to predict propeller performance degradation in icing conditions. The ice accretion code LEWICE was used to predict blade-section ice shape geometry, the RANS code Fluent was used to predict the resulting blade-section performance degradation, and a blade-element code was used to predict the corresponding propeller performance degradation. Validation data for each of these steps was available from the first two phases of the FAA investigation.

This paper is divided into three additional sections. The Computational Methods section discusses the computational tools used in this study. It is divided into three parts which discuss LEWICE, Fluent, and the blade-element code. The next section is Results and Discussion, and it is also divided into three parts: predicted ice shape geometries (which used the LEWICE code), predicted blade-section aerodynamic performance (which used Fluent), and predicted propeller performance degradation (which used a blade-element code). The final section presents the key results and conclusions of this study.

Computational Methods

The current work consisted of three stages: prediction of 2-D blade-section ice geometries using the code LEWICE, prediction of the associated blade-section aerodynamic performance degradation using the RANS code Fluent, and relation of the blade-section performance degradation to overall propeller performance degradation using a blade-element code. Each of these three stages is now discussed in more detail.

Prediction of Blade-Section Ice Geometry

The NASA-developed ice accretion prediction code LEWICE[16] was used to predict 2-D blade-section ice growth at given blade sections on the propeller blade. The main inputs to this code are blade section geometry, aerodynamic flow conditions (freestream velocity, angle of attack, etc.), and icing conditions (temperature, MVD, LWC, duration, etc.). The main output presented in this paper is ice shape geometry. This geometry was compared with ice photos

and tracings taken at three radial stations (the mid-boot, 50%, and 75% stations) during the experimental icing test at Eglin AFB. These photos and tracings are shown in Fig. 1 for three different sets of icing conditions, designated Run 3B (R3B), Run 19A (R19A) and Run 21 (R21, an SLD condition). In that test, after each icing run, an ice knife was used to slice the ice so that a template could be used to trace the ice accretion; more details on the procedure used is provided by Dumont et al.[2] Initial investigations using LEWICE during the current study showed considerable discrepancies between the tracings and the LEWICE results. It was found that these discrepancies likely resulted from ice shedding from the propeller blade and that shedding was a significant factor in this study, so some basic procedures were developed to attempt to model this phenomenon in LEWICE. These procedures are discussed in more detail in the Results and Discussion section of this paper.

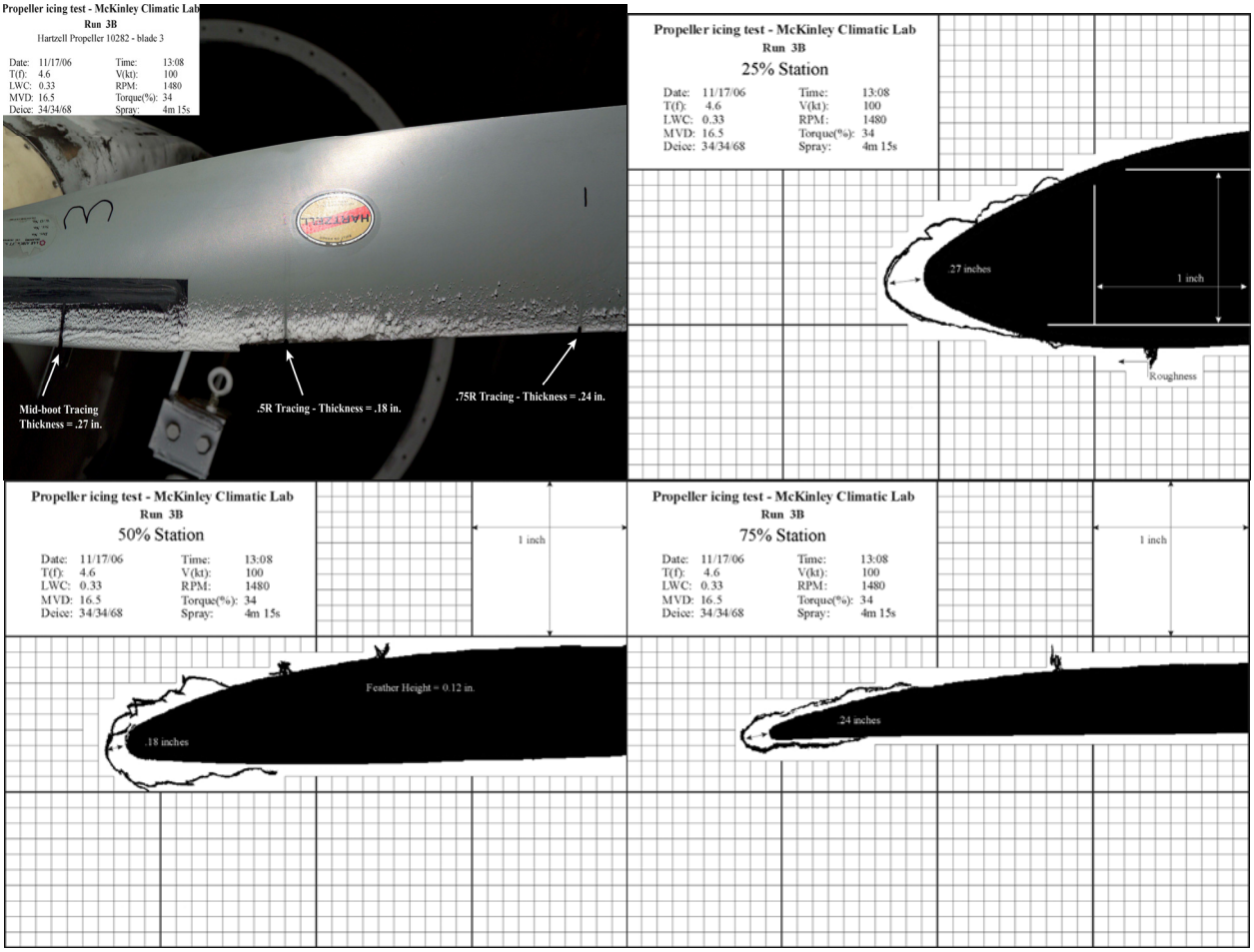

(a) Run 3B

Fig. 1 (continued on next page)

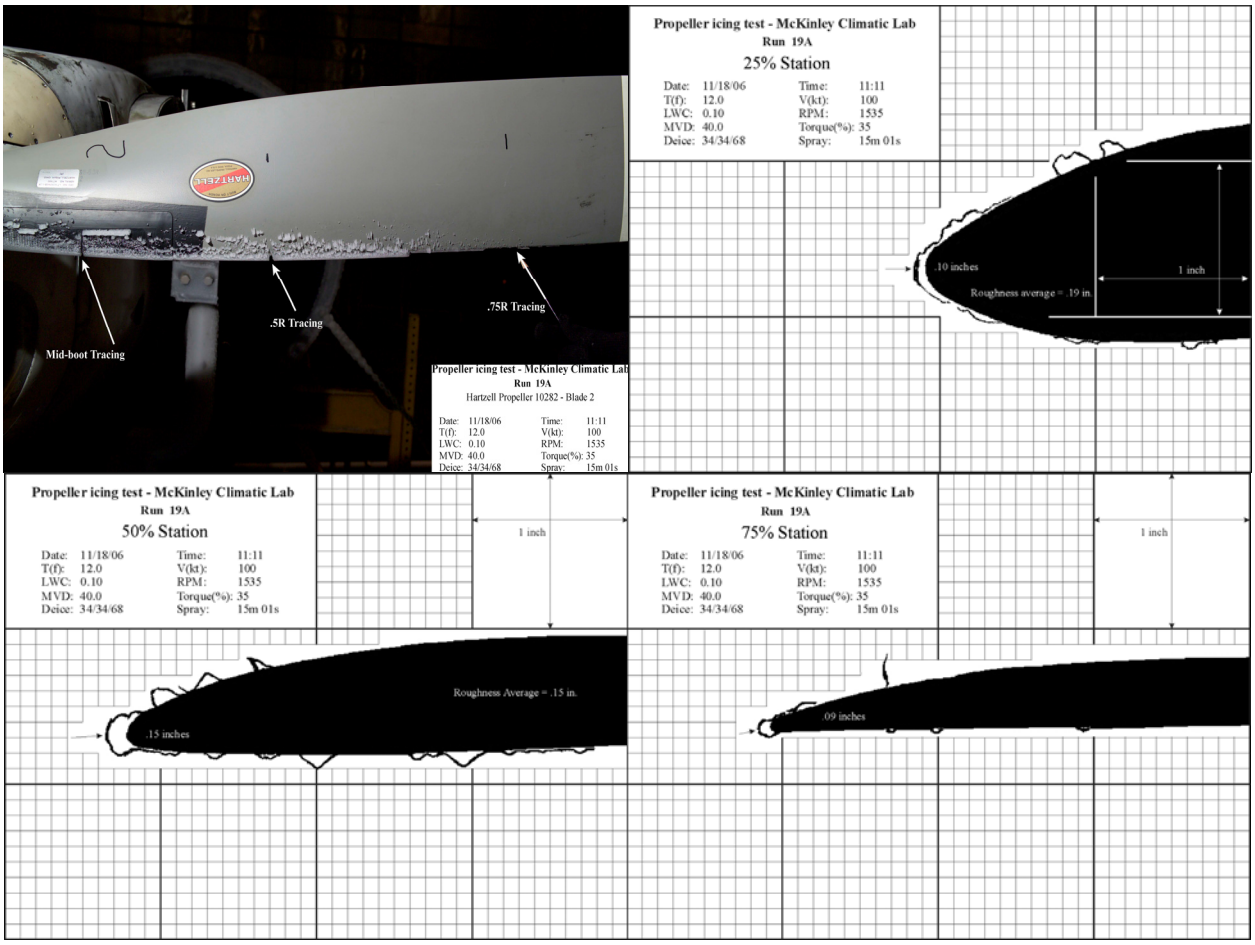

(b) Run 19A

Fig. 1 (continued on next page)

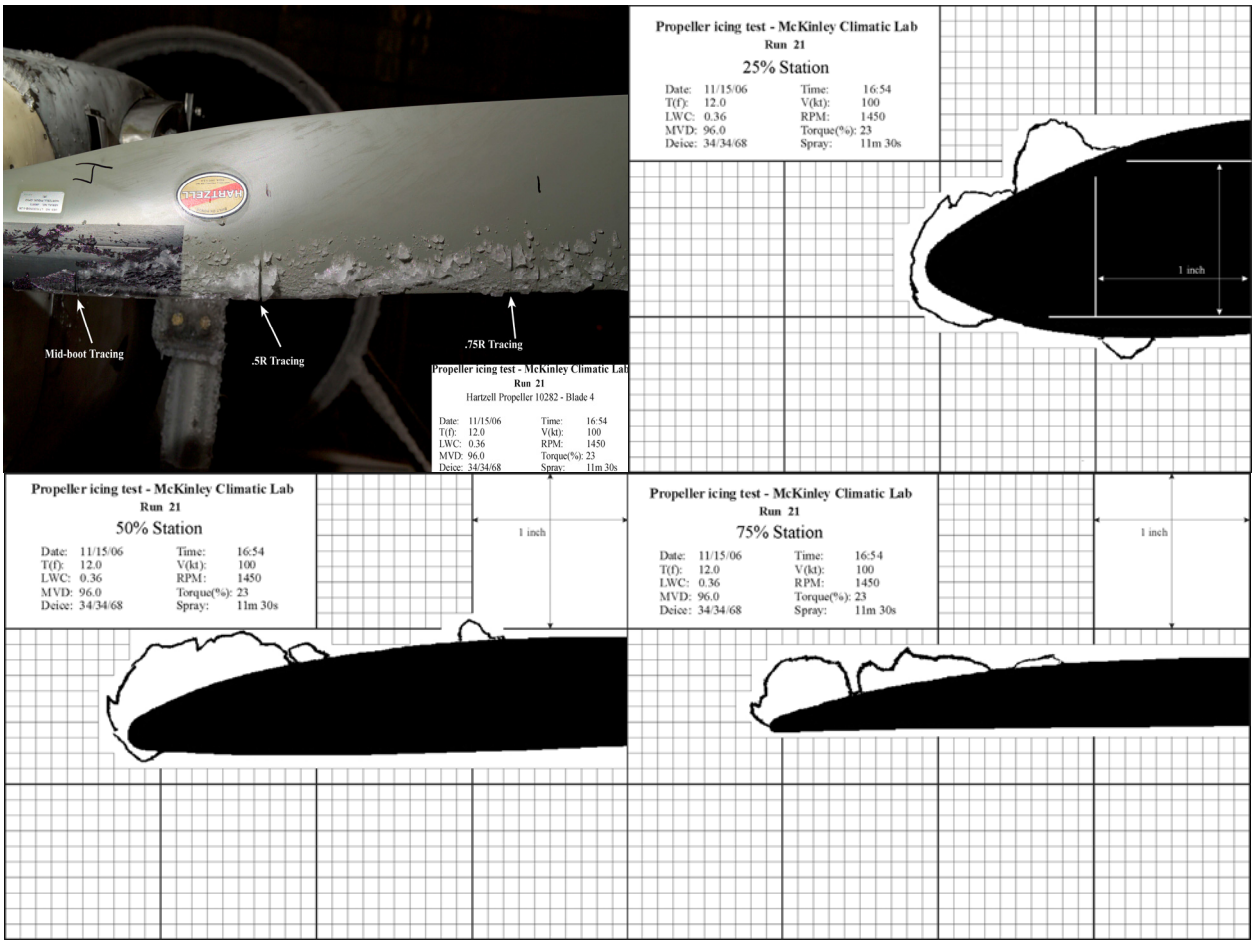

(c) Run 21

Fig. 1 Photos and tracings of ice accretions documented by Dumont et al.[2] The three tracings are for the propeller mid-boot, 50%, and 75% blade sections for the conditions of (a) Run 3B (R3B), (b) Run 19A (R19A), and (c) Run 21 (R21).

Calculation of Blade-Section Aerodynamic Performance Degradation

The commercial CFD code Fluent[17] was used to predict the iced blade-section aerodynamic performance. Fluent was used to solve the ensemble-averaged continuity and compressible Navier-Stokes equations using a finite-volume approach. Fluent was run in 2-D double-precision mode, and the equations were solved using the pressure-based solver with the Green-Gauss node-based gradient option. Interpolations across cells were performed using 2nd order accuracy for pressure and the 3rd order MUSCL scheme for the momentum and modified turbulent viscosity discretizations. The SIMPLEC algorithm was used to couple pressure and velocity.

To model turbulence, the one-equation Spalart-Allmaras (S-A) turbulence model[18] was used for all cases, as Chung and Addy[19] and Chi et al.[20] showed that this model could provide accurate results for airfoils with rime ice until near airfoil $C_{l,max}$. No turbulence models were found to accurately predict the $C_{l,max}$ and post-stall characteristics of glaze ice due to the large regions of separated flow that result from these accretions, but the S-A model was among the best tested by Chi et al. Each airfoil was modeled assuming completely turbulent flow due to the lack of transition location data and to reduce the number of meshes required for this study. While modeling boundary-layer (or shear-layer) transition may have had an effect on the results, no data regarding transition location on the relevant airfoil/ice geometries were available for this study. Techniques such as the improved Michel's Criterion[21] were investigated to use Fluent to predict the transition location. However, when these techniques were validated on an iced-airfoil with a known transition location (based on the data of Jacobs[22]), they were not found to be very accurate. It was beyond the scope of this study to further investigate or develop transition-prediction techniques, so the flow was assumed fully turbulent. This decision was also made to reduce the computational time

required for these calculations, as accounting for transition would have required that a new mesh be made for every configuration at each angle of attack, increasing the number of required meshes by an order of magnitude.

Meshes were constructed for Fluent using Gambit,[23] and a sample mesh is shown in Fig. 2. For each case, an inner and outer mesh was used, both of which were structured and used quad elements. The inner mesh surrounded the airfoil to a distance of one chord length, and the outer mesh extended ten chord lengths upstream of the airfoil, twenty chord lengths downstream of the airfoil, and about ten chord lengths above and below the airfoil. These extents were confirmed to be sufficient by performing a trade study which increased the mesh extents, and the relevant performance parameters were identical with the larger mesh. Fluent was used to adaptively refine the mesh to limit the magnitude of the maximum velocity gradient using a refine threshold of 10% and to ensure that y+ remained less than 5 nearly everywhere on the airfoil surface. This value was suggested to be the maximum acceptable in the Fluent User Manual,[24] as the Fluent S-A model is modified to use wall functions so y+ values between 5 and 30 should be avoided to maximize accuracy. A y+ value greater than one was necessary to avoid very fine meshes, as y+ may vary greatly on iced-airfoils due to the highly irregular geometry and achieving a y+ = 1 everywhere on the airfoil surface for every mesh was impractical for this study. A sensitivity study was performed on a single mesh (the iced 50% blade-section for the shape of R3B) to ensure that maximum y+ values of less than 5 were adequate, and the solution did not appear to be significantly affected by reductions in y+ below 5.

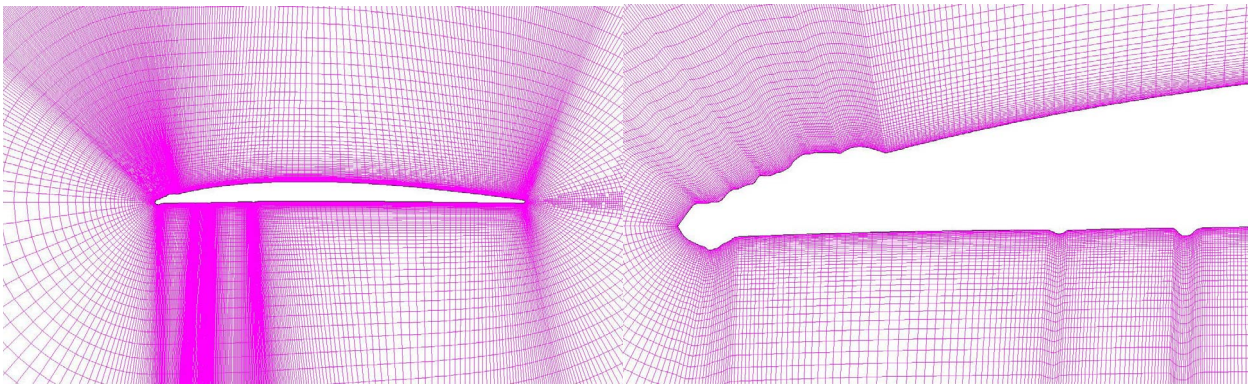

(a) (b)

Fig. 2 Sample mesh used for the Fluent calculations: (a) mesh around the entire blade-section geometry and (b) close-up of the mesh around the ice shape. This mesh was used for the 75%-station blade-section for the icing conditions of R19A.

Due to large uncertainties encountered due to ice shedding, the experimental ice tracings were analyzed in Fluent instead of the LEWICE-predicted ice geometries (this is discussed more in the Results section). These tracings, shown in Fig. 1, were smoothed using 25% control points in SmaggIce[25] to reduce the required mesh size. Chung et al.[26] suggested that smoothing down to 50% control points gives results comparable to using 100% control points, but further smoothing may affect the predicted aerodynamic performance. However, this is in part dependent upon the density of points in the digitized tracing. In this study, the tracing digitizations were very dense, and using 25% control points altered the tracing geometry a qualitatively similar amount to 50% control points in the study of Chung et al. Since only the ice tracings were digitized (and not the clean blade sections), the digitized tracings had to be matched to the clean blade section coordinates. Due to inaccuracies in the tracing process, the ice tracing coordinates did not always align with the clean airfoil coordinates. To match the ice geometry to the clean airfoil, the ice geometry coordinate closest to the clean airfoil surface (and above the surface) was connected to the closest clean airfoil coordinate downstream of the ice shape.

Calculation of Icing Effects on Propeller Performance

During an earlier part of this study, a propeller performance code was developed using the blade-element and vortex theory methods described by McCormick.[27] Blade-element theory discretizes the propeller blade radially into thin blade sections. Given the propeller geometry and the aerodynamic performance characteristics of each blade section, the incremental thrust and power coefficients dC_T and dC_P can be obtained as a function of known quantities and the induced angle of attack α_i on each blade section (eqs. 1 and 2). Once the induced angle of attack is known, the incremental thrust and power coefficients can be integrated across the propeller blade and multiplied by the number of blades to compute the propeller thrust and power coefficients.

$$dC_T = (J^2 + \pi^2 x^2)\sigma[C_l \cos(\phi + \alpha_i) - C_d \sin(\phi + \alpha_i)] \quad (1)$$

$$dC_P = \pi x(J^2 + \pi^2 x^2)\sigma[C_l \sin(\phi + \alpha_i) + C_d \cos(\phi + \alpha_i)] \quad (2)$$

Vortex theory is used to obtain the induced angle of attack on each blade section. The theory assumes that the propeller blade trailing vortices lie along a helical path of constant pitch in the propeller ultimate wake. Combining this assumption with the Kutta-Joukowski theorem and a second assumption that the induced velocity w is normal to the resultant velocity V_E, the induced velocity (and thus α_i) at each blade section can be related to the local section lift coefficient C_l. However, since C_l is dependent on α_i, an iterative scheme is necessary to solve for α_i. Once α_i is known, blade-element theory provides propeller C_T and C_P, as described above. Tip losses are accounted for using Prandtl's tip-loss factor, which drives the section lift coefficient to zero at the blade tip. More details of this code are documented by Krug[28] and Busch, Bragg, and Broeren.[3]

Results and Discussion

The results section of this paper is divided into four parts. The first part briefly describes the run conditions of the icing test by Dumont et al.[2] which were investigated in the current study. The next part discusses LEWICE-predicted ice geometries at the mid-boot, 50%, and 75% propeller blade sections for each of the three runs shown in Table 1. The third part discusses blade-section aerodynamic performance predicted using Fluent. The final section discusses propeller performance calculations made using these aerodynamic performance data and the propeller performance code discussed earlier in the paper.

Run Conditions

As discussed in the Introduction, Dumont et al.[2] conducted a full-scale propeller icing test in the McKinley Climatic Laboratory at Eglin AFB and documented ice accretions formed at the mid-boot, 50%, and 75% blade stations for several run conditions. Three of these run conditions, listed in Table 1, were chosen to investigate using the propeller performance code discussed above. Note that the McKinley test was conducted at a freestream velocity of 100 kts, which is substantially below the freestream velocity for in-flight conditions. Therefore, the flight-condition blade section angle of attack could only be matched at a single radial station. This target angle of attack and the corresponding test location are given in Table 1. The conditions of Runs 3B and 19A are Appendix C conditions, while Run 21 is an SLD condition. Fig. 1 shows the ice accretion photos and tracings taken from Dumont et al.[2]

Table 1 Summary of run conditions used by Dumont et al.[2] for which ice accretions were simulated in the present study.

Run	LWC (g/m^3)	MVD (μm)	OAT (F)	Spray Time	Target α (deg)	Radial Location of Target α	Pitch, x = 0.61 (deg)	Torque (%)	RPM
3B	0.33	16.5	4.6	4 min 15 s	0.5	0.75	26.2	34	1480
19A	0.10	40	12.0	15 min 1 s	2.0	0.25	26.2	35	1535
21	0.36	96	12.0	11 min 30 s	2.0	0.25	25.1	23	1450

Predicted Ice Geometries

As discussed in the Computational Methods section, LEWICE has been validated to predict 2-D ice geometries on 2-D airfoil sections. It requires as inputs the airfoil section (or in this case, blade section) on which ice will be accreted, the flow conditions, and the icing conditions. The clean propeller blade geometry is known and the icing conditions for a given run are summarized in Table 1. The flow conditions at each radial station were determined with a blade-element code using clean and iced blade-section aerodynamic performance experimentally obtained using artificial ice shapes by the authors in an earlier part of this study.[3] Ordinarily, the flow conditions at each radial station would not be known, as they would depend on the ice geometry along the propeller blade (which depends on the flow conditions, and so on). Thus, without experimental data, an iterative process coupling

LEWICE, Fluent, and a propeller performance code (e.g., a 2-D strip method) would have to be used to obtain the proper flow conditions to use as an input to LEWICE. This procedural difference has no effect on the results presented since the LEWICE geometries were never analyzed using Fluent due to uncertainties regarding ice shedding effects; this will be discussed in more detail later in this paper.

The LEWICE-predicted ice geometry for the 75% radial station blade section and the icing conditions of Run 19A is compared with the actual ice geometry (as determined from an ice tracing) in Fig. 3. The ice geometry predicted by LEWICE is much larger than the experimentally observed geometry. LEWICE predictions for other blade sections under other icing conditions were generally consistent in over-predicting the mass of ice accreting on the airfoil surface. Many of these predicted geometries appeared un-physical in that they would likely not be able to withstand the loading encountered on a rotating propeller blade, so stop-action video of the icing test was examined to determine if ice was shed during the test. Fig. 4 shows a sequence of images obtained from this video (for Run 19A), beginning just prior to the first shed event and ending after the last shed. In the images, the propeller blade is moving from right to left, and the propeller hub is located near the top of each image. The dark area of the propeller blade near the top of each image is the de-icing boot, and ice accretion (white) is visible on the left side of each blade (near the leading edge). After the first image, each subsequent image was obtained after a shedding event. (Note that some of these events can be difficult to discern in the figure.) For example, the second photo from the left shows an ice shed from about $x = 0.65$ to 0.75 which occurred about 4 min. and 34 s into the run, and the third photo shows another ice shed from about $x = 0.55$ to 0.65 which occurred about 5 min and 40 s into the run. Throughout the sequence, ice can be seen to accrete a second time in this region, but it is shed again in the last photo, just prior to the end of the run.

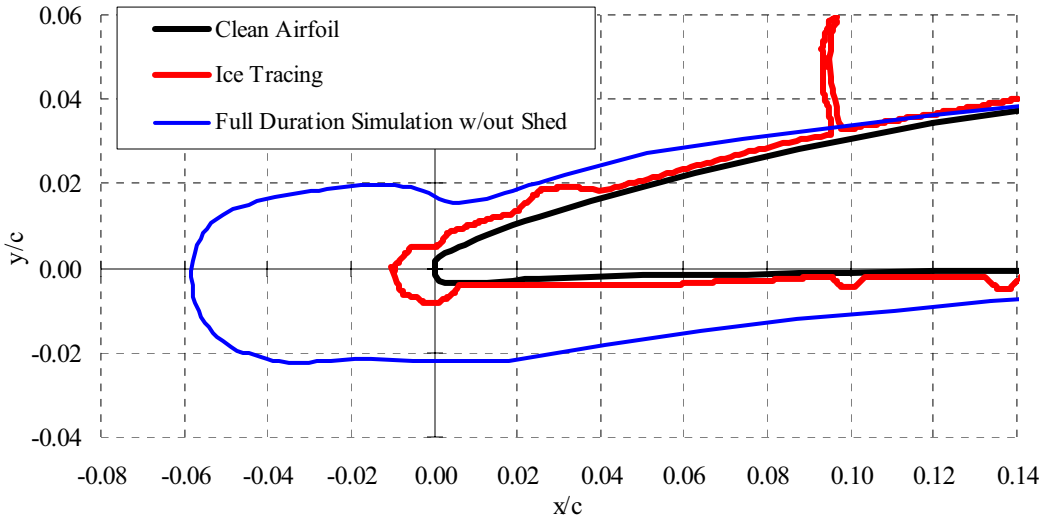

Fig. 3 Comparison of LEWICE predicted ice geometry with experimental ice tracing for the 75% blade station and the icing conditions of Run 19A.

To improve the fidelity of the LEWICE predictions, a procedure was developed to help account for the ice shedding events. Since there are currently no reliable, validated methods for accurately predicting ice shedding on propeller blades, stop-action video from the experimental icing test (such as that shown in Fig. 4) was used to determine the extent, frequency, and approximate time of shedding for each icing run. Note that to computationally predict propeller ice accretion geometry without supporting experimental data, an accurate shedding model would need to be developed.

Two types of shed events could occur during the icing test at a given radial station: a complete shed of all ice or a partial shed of ice, in which some ice remained on the blade surface after the shed event (usually at reduced chordwise extents). To predict ice geometry at a blade station which experienced a complete shed, an "effective" icing encounter duration was introduced which was equal in length to the difference in time between the last complete shed at the relevant blade station and the end of the run. LEWICE was then used to predict the blade-section ice geometry, starting with the clean blade section (essentially the geometry resulting from a clean shed) and using the "effective" run time as the icing encounter duration.

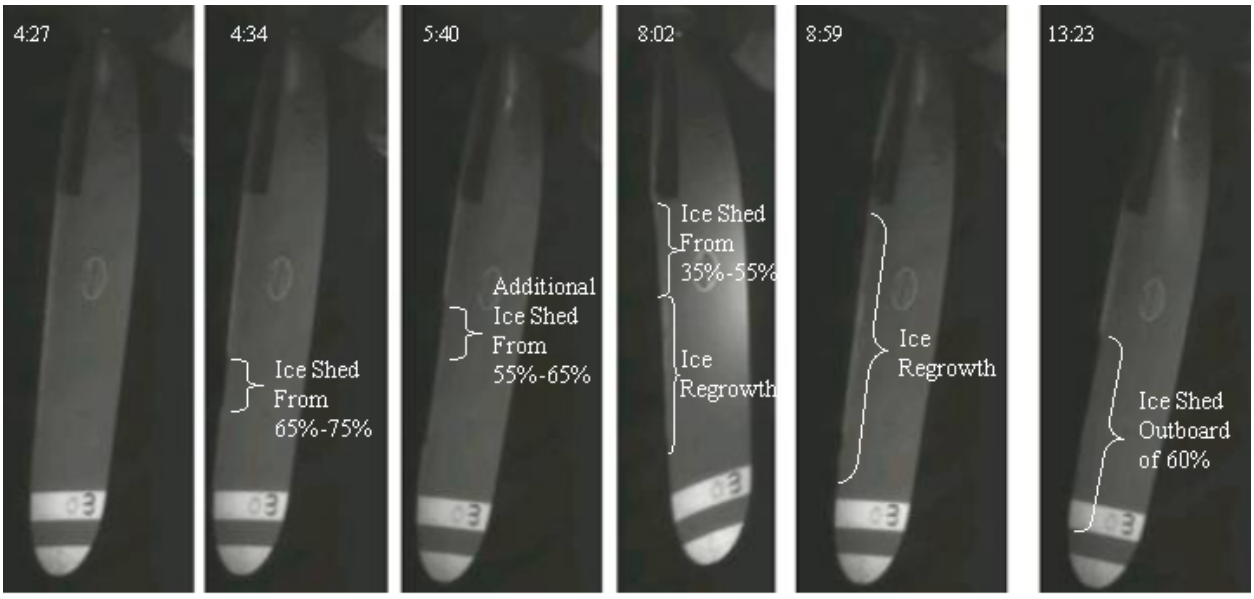

Fig. 4 Images obtained from stop-action video of Run 19A icing test showing evolution of ice growth and shed events.

The Run 3B case at the 75%-station is given as an example in Fig. 5. In this case, the 75% blade station experienced a complete ice shed 93 s into the icing test. Therefore, LEWICE was run for the duration of the test (162 s) using the clean 75%-station blade-section geometry as the input. This resulted in the geometry labeled "Final Shape with Shed" in Fig. 5, and it compared reasonably well with the ice tracing obtained immediately after the icing test. For comparison, the much larger LEWICE-predicted geometry which did not account for ice shedding is also shown in Fig. 5 (labeled "Final Shape Assuming No Shed").

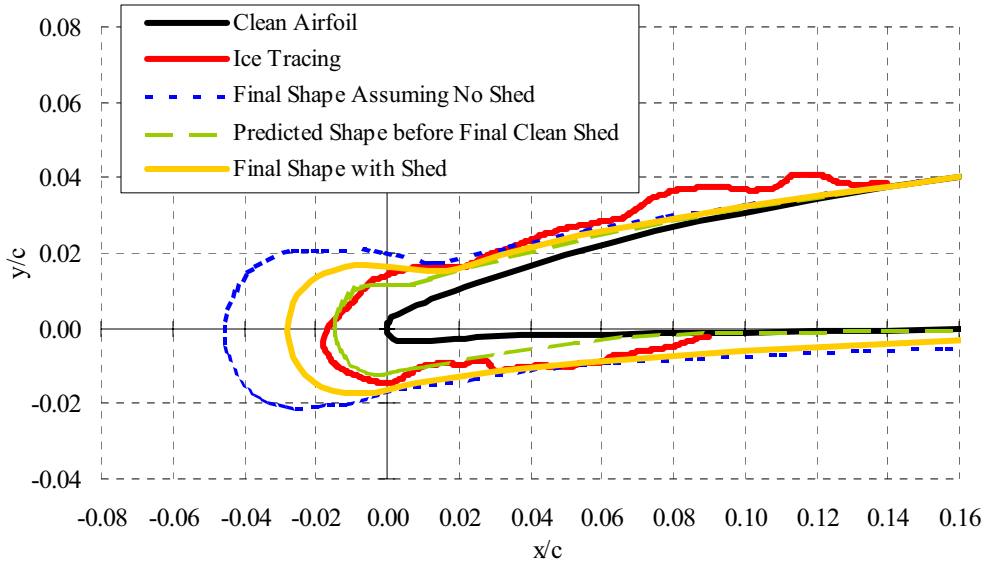

Fig. 5 LEWICE-predicted ice geometry using the complete ice-shedding procedure for the 75%-station blade section for the icing conditions of Run 3B.

While complete ice sheds occurred in several cases, many times the ice only partially shed, leaving smaller chunks of residual ice on the propeller blade. In these cases, the only documentation of the ice geometry resulting from the shed is stop-action video, and the detailed ice cross section can not be determined. This presents a limitation to the effectiveness of LEWICE in predicted the final ice geometry, as the final ice geometry is very

sensitive to the geometry immediately following the shed. To determine if LEWICE could predict the final ice geometry reasonably well if measurements had been taken of the post-shed geometry, LEWICE was run using the clean blade section as the geometry input for the duration of time between the beginning of the icing run and the partial shed. At this point, just prior to the shed, the LEWICE-predicted geometry was compared with ice tracings obtained at the end of the icing test to determine a likely post-shed ice cross section. This cross section was then used as the input for a second LEWICE run, and, as with the complete shed case, an "effective" icing encounter duration was introduced which was equal in length to the difference in time between the partial shed at the relevant blade station and the end of the run. For cases in which more than one partial shed occurred, only the final partial shed was analyzed. Also, for consistency, whenever partial shedding took place, it was assumed that the ice shed all the way through to the propeller blade surface. To summarize, this procedure is outlined in a step-by-step process below, using the mid-boot station blade section for the conditions of Run 21 (Fig. 6) as an example.

1) Starting with the clean airfoil, LEWICE was run until the final (or only) occurrence of partial shedding was observed in the stop-action video. (For the mid-boot station in Run 21, this occurred 571 s into the run, and the predicted shape at this point is labeled "Predicted Ice Shape before Final Shed")

2) Based on the ice tracing, ice was removed over certain chordwise extents (down to the airfoil surface), and this modified shape was input into LEWICE as the new geometry input. (For the mid-boot station in Run 21, this post-shed geometry is labeled "Assumed Ice Shape after Final Shed" in Fig. 6.)

3) LEWICE was run a second time with the estimated post-shed geometry for the remaining duration of time in the run. (The final LEWICE-predicted ice geometry is labeled "Final Shape with Shed" in Fig. 6 for the mid-boot station in Run 21.)

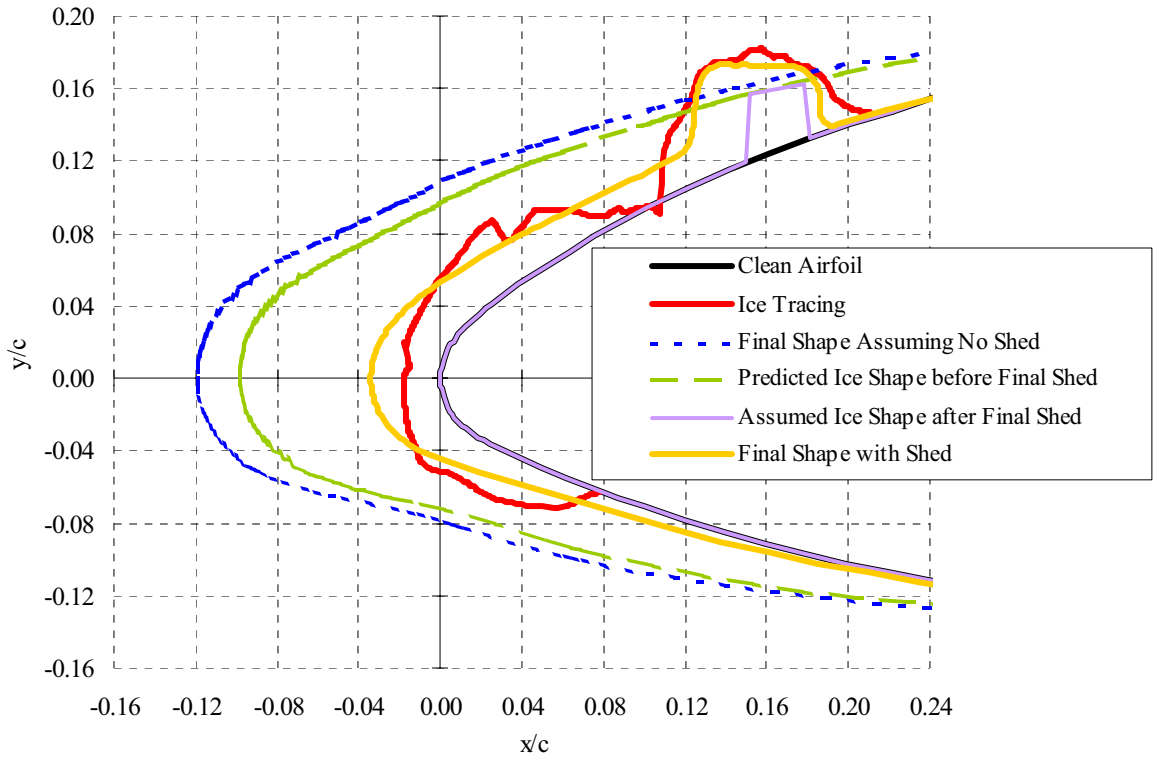

Fig. 6 LEWICE predicted ice geometry using the partial ice-shedding procedure for the mid-boot blade section for the icing conditions of Run 21.

This procedure gave results that were in reasonably good agreement with ice tracings immediately after each icing test (Fig. 6). LEWICE predicted a similar amount of mass of ice to accrete on the airfoil as was measured during the

test, and for the example shown in Fig. 6, the large horn-like feature on the upper surface was appropriately captured. These trends were consistent for most of the other cases investigated.

This study showed that the unusual geometries on the propeller blades observed at the end of the icing tests were caused by the shedding of ice during the test, and it is likely that LEWICE can at least qualitatively reproduce these geometries if the ice geometry immediately after the shed is known. Due to the large uncertainties inherent in the prediction of ice shedding on rotating propeller blades and the associated uncertainties in the LEWICE predictions, the LEWICE geometries were not used in the second phase of the study, which used Fluent to determine iced-blade section aerodynamic performance. Instead, the experimentally obtained ice tracings were smoothed and used as the geometry inputs to Fluent (discussed next). It is recommended that additional research regarding ice shedding be conducted to develop an accurate shedding model. With such a model, LEWICE could potentially be used with better accuracy and the need for experimental ice geometry data would be greatly reduced.

Predicted Blade-Section Aerodynamic Performance

This portion of the study was conducted to determine the aerodynamic performance degradation of the mid-boot, 50%, and 75%-station propeller blade-sections due to ice accretion using the RANS code Fluent. Due to the difficulties in using LEWICE to predict blade-section ice geometry (discussed above), ice tracings obtained during the experimental icing test at Eglin AFB (discussed in the Introduction) were used as the inputs to Fluent. These ice tracings, shown in Fig. 1, were smoothed using 25% control points to reduce computation time (as discussed in the Computational Methods section).

For the blade sections at each of the three radial stations of interest (the mid-boot, the 50%, and the 75% stations), the clean and iced blade-section aerodynamic performance data predicted by Fluent are shown in Fig. 7 and compared to the blade section aerodynamic performance experimentally measured using artificial ice shapes in an earlier phase of this investigation and discussed in more detail in Reference 3. Due to time constraints, for each blade station, only angles of attack in the range experienced during the icing test at Eglin AFB were analyzed in Fluent. Iced data are shown for three sets of icing conditions, designated R3B, R19A, and R21, which are summarized in Table 1.

The effect of ice accretion on the aerodynamic performance of the mid-boot blade section is shown in Fig. 7(a) for each of the runs R3B, R19A, and R21. The clean blade-section performance predicted by Fluent is considerably worse than the experimentally-measured clean performance; the lift curve slope has a slightly lower slope and is shifted about 3 deg., resulting in a predicted value of C_l about 0.2 lower than what was measured at a given angle of attack using artificial ice shapes. This discrepancy is not surprising since in the earlier, experimental portion of this study, the 33% thick mid-boot blade section was found to be extremely sensitive to surface condition[3] and the thick root section of wind-turbine blades exhibit similar characteristics.[29] Two-dimensional trip strips of width s/c = 0.023 and height k/c = 0.00056 located at x/c = 0.10 on the upper and lower surface caused radical changes in the lift curve slope, similar to those shown in Fig. 7(a) due to the (experimentally measured) effects of ice. For the Fluent runs, the flow was considered to be completely turbulent, since no data were available regarding transition location and to reduce the required computation time (this is discussed more in the Computational Methods section).

The Fluent-predicted iced blade-section aerodynamic performance is also shown in Fig. 7(a). As would be expected given the sensitivity of the mid-boot section to surface roughness, ice accretion substantially degraded blade section performance. Fluent showed that the R3B ice shape caused a smaller penalty than the shapes of R19A or R21, although the shape still had a large effect. According to Fluent, the ice shape caused a slight decrease in the lift curve and caused it to shift about 2 deg. to the right. This penalty, while large, was not as large a penalty as that measured using an artificial ice shape to represent the R3B accretion (Fig. 7(a)). The Fluent predictions for the ice shapes of R19A and R21 were also in poor agreement with experimental results. Much of the flow over the airfoil was separated, and a short-coming of RANS codes is that their accuracy tends to diminish in unsteady, highly separated flowfields such as the flowfield about the mid-boot blade section with ice accretion.

Fluent predictions for the clean and iced 50%-station aerodynamic performance are shown in Fig. 7(b). The clean 50%-station blade section performance predicted by Fluent was in considerably better agreement with experiment than was the case for the mid-boot section (this 9%-thick airfoil geometry was also much less sensitive to surface contamination). Fluent predicted a $C_{l,max}$ of about 1.0, while the experimentally-measured $C_{l,max}$ was just below 1.2. Fluent also predicted a steeper lift curve slope *and* $C_{l,max}$ to occur at a 2 deg. lower angle of attack. The agreement in C_d was reasonably good over the range α = 3 to 11 deg.

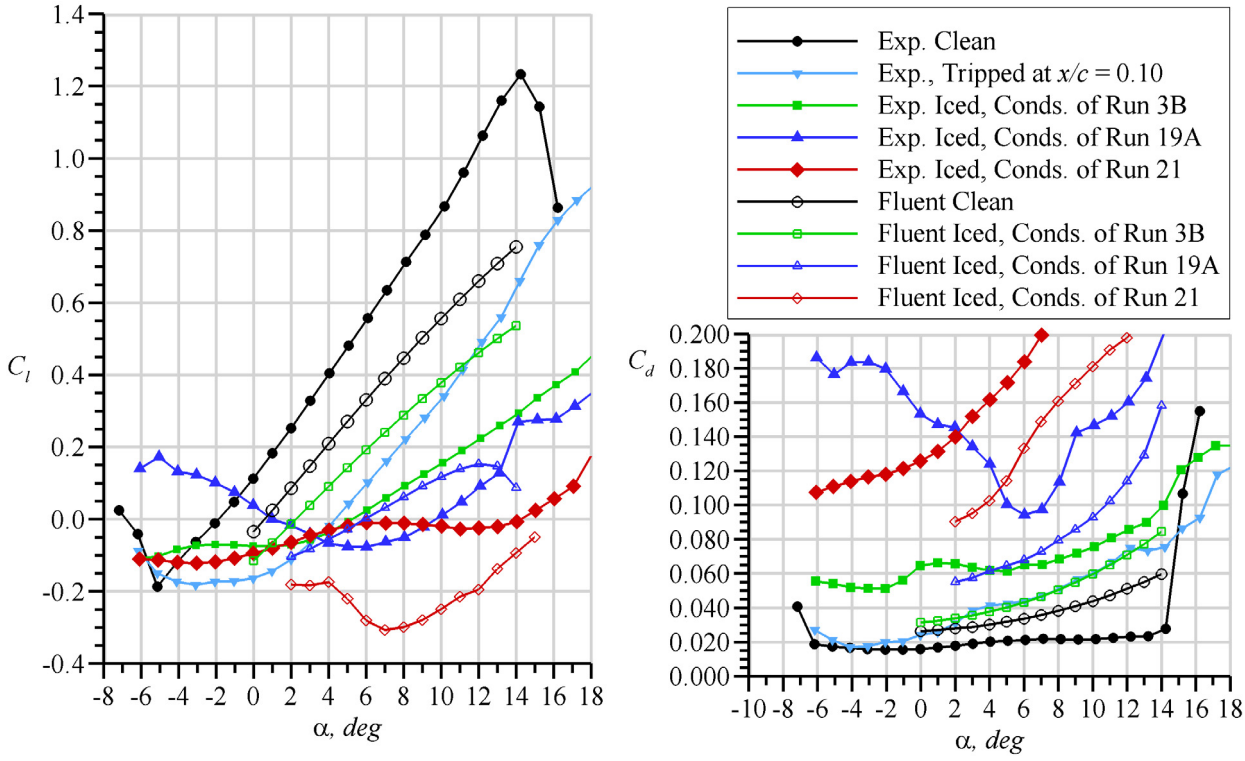

(a) mid-boot station blade-section performance

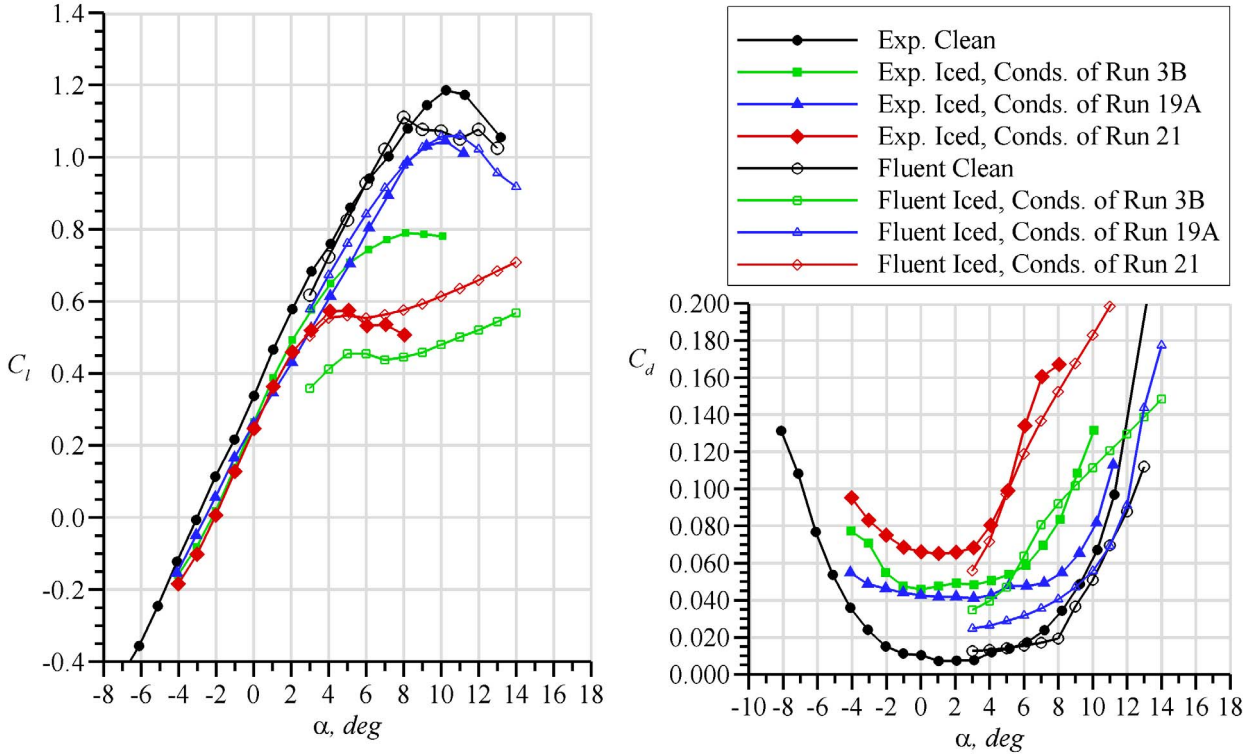

(b) 50%-station blade-section performance

Fig. 7 (continued on next page)

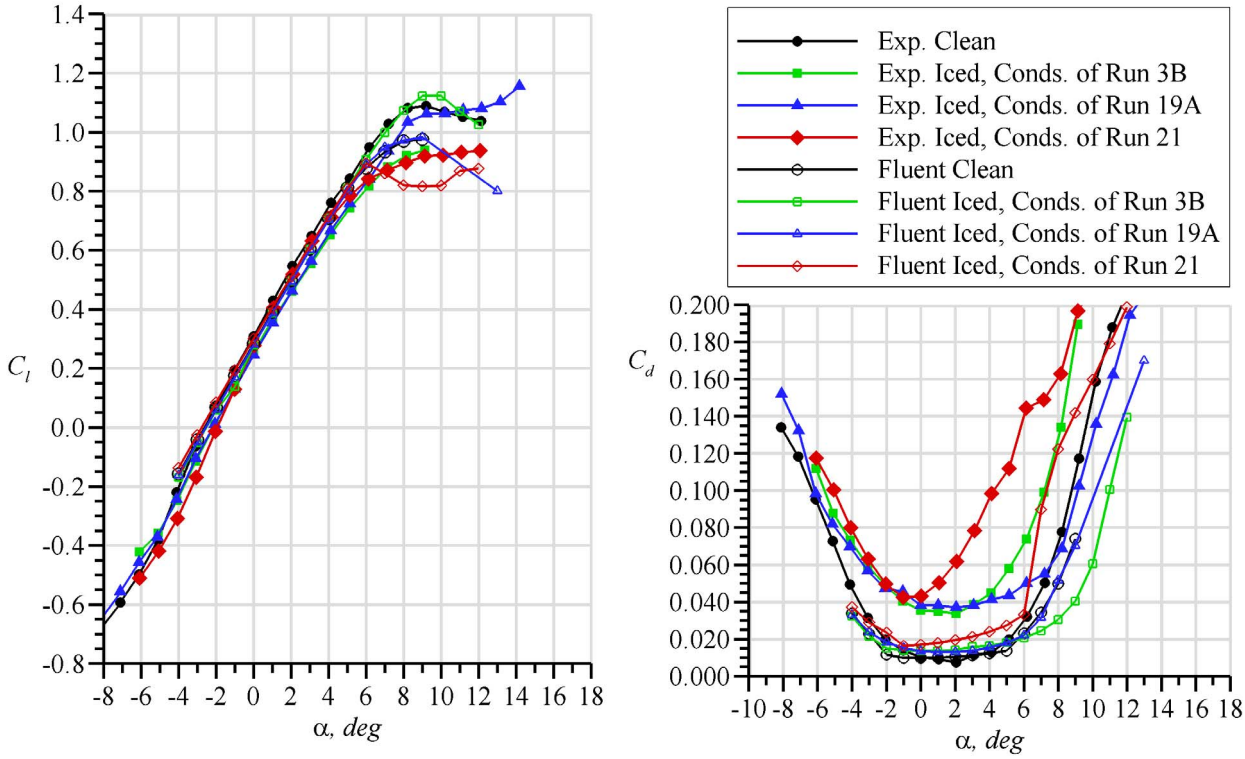

(c) 75%-station blade-section performance

Fig. 7 Comparison of experimentally-measured and Fluent-predicted clean and iced blade-section aerodynamic performance for the (a) mid-boot, (b) 50%, and (c) 75% radial stations.

Ice accretion had a large effect on the aerodynamic performance of the 50% station blade section (Fig. 7(b)) though not as large as on the mid-boot section. According to the experimental data, the R21 ice shape caused the largest decrease in $C_{l,max}$ and the largest increase in C_d, while the R19A ice shape had the smallest effects. Fluent showed similar trends for C_d, but predicted the R3B shape to cause a larger $C_{l,max}$ penalty than the R21 shape. Note that the range of angle of attack for which Fluent data were obtained in the R3B and R21 cases was near $C_{l,max}$ and in the post-stall regime. This range of angle of attack was representative of the operating conditions of the propeller blade at the low freestream velocity of 100 kts used in the Eglin icing test. At true flight conditions, the freestream velocity would be closer to 240 kts and the propeller blade would operate at lower angles of attack. At the high angles of attack for which these data were obtained, there was likely a large degree of unsteadiness and flow separation in the iced-airfoil flowfield.

The 75%-station blade section, which was less than 6% thick, exhibited the least sensitivity to ice accretion, especially in regard to $C_{l,max}$ (Fig. 7(c)). Fluent predicted a clean blade-section $C_{l,max}$ of just 1.0 at α = 9 deg., compared with an experimentally-measured value of about 1.08 at the same angle. Better agreement was observed between the Fluent and experimental results for C_d, which was very similar over most of the angle of attack range investigated.

The R21 ice shape was the only one predicted to cause a decrease in $C_{l,max}$; the ice shape of R19A had negligible effect on $C_{l,max}$ and the ice shape of R3B was predicted to cause an increase in $C_{l,max}$ (Fig. 7(c)). This was likely due to an increase in the "effective" blade section chord length due to ice accretion on the leading edge (Fig. 1(a)) or the ice shape may have acted as a leading-edge flap. Increases in $C_{l,max}$ have also been documented in previous studies on ice shapes with similar geometries.[30] While Fluent predicted an increase in $C_{l,max}$ due to the R3B ice shape, experimental measurements on an artificial ice shape showed a decrease in $C_{l,max}$ of about 0.15. This discrepancy may in part have been due to the use of grit roughness on the artificial ice shape, whereas the 2-D Fluent model only incorporated the two-dimensionalized roughness present on the ice tracing. The drag coefficients predicted by Fluent for each of the three icing cases also tended to be significantly lower than those measured experimentally, especially at low angle of attack.

Predicted Propeller Performance

Once the clean and iced blade-section aerodynamic performance were known, the overall propeller performance degradation in icing conditions was calculated using a blade-element code (described in more detail in the Computational Methods section of this paper). The results are shown in Fig. 8 - Fig. 13. Data obtained during the first and second phases of the FAA investigation, described in the Introduction, are also shown for comparison. Recall that propeller performance degradation in the first phase was measured experimentally in an icing test at Eglin AFB, and the propeller performance degradation in the second phase was determined using a blade-element code (the same used in the current study) and based on experimental wind-tunnel measurements of blade-section aerodynamic performance degradation using artificial ice shapes. The propeller performance data obtained during the current study (the third phase) was calculated from a blade-element code and based on blade-section aerodynamic performance obtained from two-dimensional Fluent analyses of ice shapes traced during the Eglin AFB icing test; LEWICE-predicted ice geometries were not used due to uncertainties in the ice shedding process, as discussed in the section entitled Predicted Ice Geometries. During the icing test, propeller performance data were measured only at one advance ratio, so the experimental data is shown as a single point. Propeller performance data obtained during the second and third phases of this study are shown at multiple advance ratios to show trends at different operating conditions.

In Fig. 8(a), which shows the results for the icing conditions of Run 3B (detailed in Table 1), an experimentally-measured clean propeller C_T of about 0.228 and an iced propeller C_T of 0.214 are shown, both at $J = 0.82$. Thrust data calculated during the second phase of the FAA investigation shows a lower clean propeller $C_T = 0.207$ and iced propeller C_T of 0.184; recall that these data used blade section aerodynamic performance data experimentally measured using artificial ice shapes, and a blade-element code to relate blade-section performance to propeller performance. Data obtained during the current study, which used Fluent to determine blade-section aerodynamic performance and the same blade-element code used in the second phase, shows a clean propeller $C_T = 0.206$ and an iced propeller $C_T = 0.178$. These values are below the experimentally-measured values by 10% and 17%, respectively. Measured and predicted clean and iced propeller C_P and η are shown in Fig. 8(b) and (c). These plots show slightly better agreement between experimental and computational values. In all cases, both C_P and η were predicted to decrease. As with C_T, the experimentally-measured C_P and η tended to be higher than the predicted C_T for both the second phase of the FAA investigation and the current study.

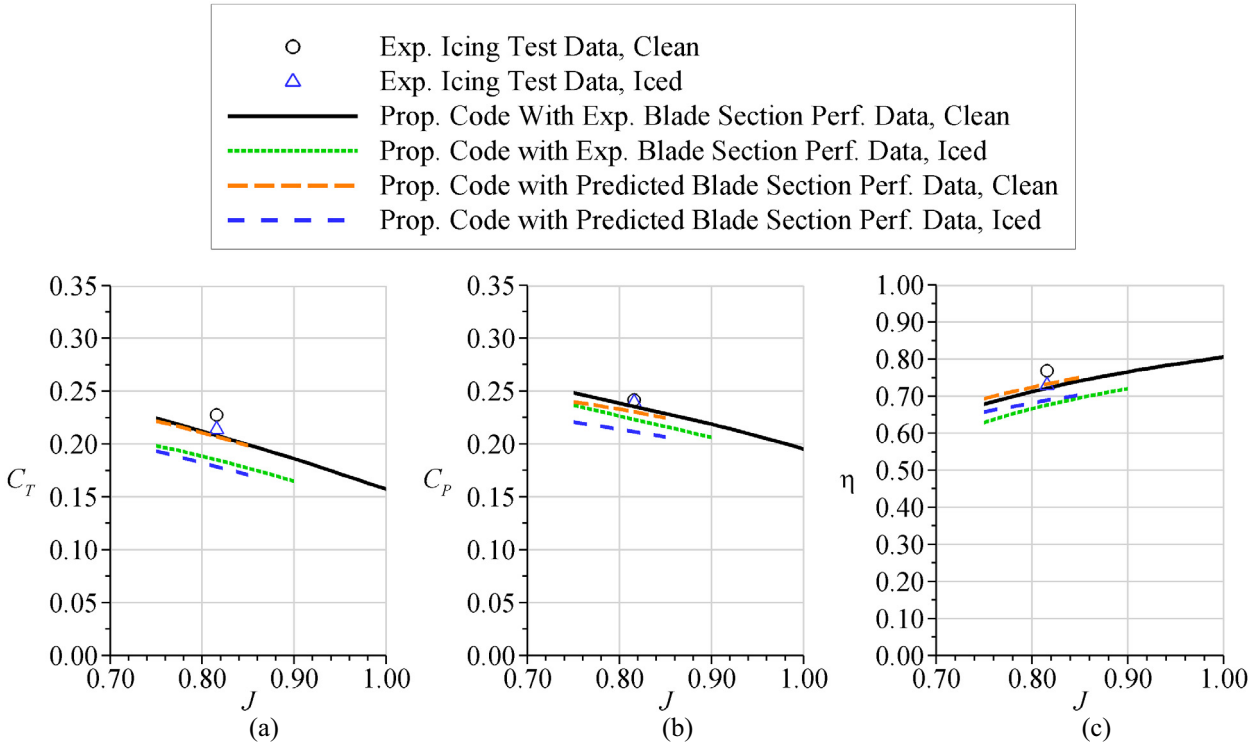

Fig. 8 Comparison of measured and predicted propeller (a) thrust coefficient, (b) power coefficient, and (c) efficiency for the icing conditions of Run 3B.

Another useful comparison between the experimental and computational data is the percent degradation in propeller performance. This is illustrated in Fig. 9. The experimentally-measured percent reduction in C_T was about 6%, compared with 11% and 14% for the second phase and current study results, respectively. Similarly, the computational methods predicted a larger degradation in C_P than observed: the second phase and current study predicted C_P reductions of 5% and 8% at $J = 0.82$, compared with a measured reduction of only 1%. The differences between measured and predicted C_T and C_P mostly canceled out in the calculation of η ($\eta = J*C_T/C_P$), resulting in agreement to within about 1% efficiency drop at $J = 0.82$ among the different methods of determining η.

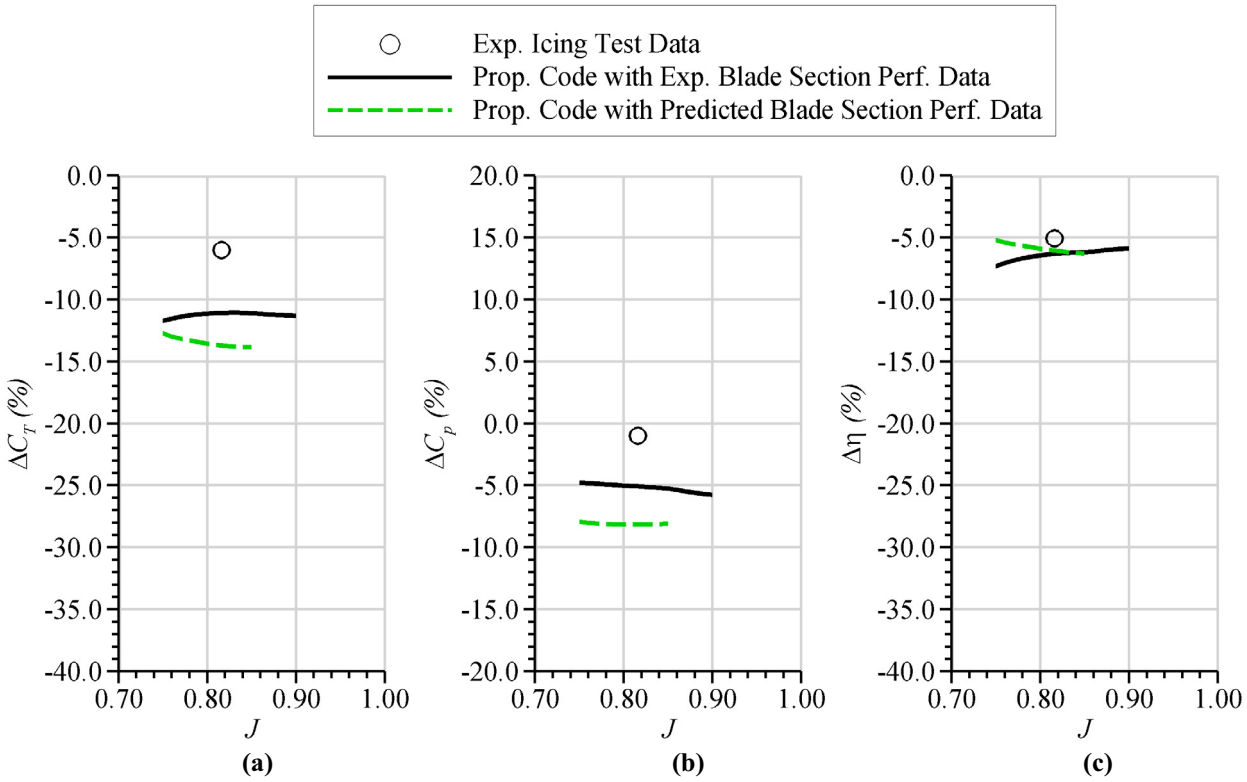

Fig. 9 Comparison of the measured and predicted change in propeller (a) thrust coefficient, (b) power coefficient, and (c) efficiency due to ice accretion from the icing conditions of Run 3B.

Analogous plots are shown for the icing conditions of Run 19A in Fig. 10 and Fig. 11. Agreement was much better between the measured and Fluent/blade-element code predicted clean propeller performance than was the case for Run 3B, with C_T, C_P, and η within about 2% at $J = 0.78$. Agreement in iced propeller performance was also better than for the conditions of Run 3B, with differences of 7%, 3%, and 4% for C_T, C_P, and η between the experimentally-measured performance and the performance computed using Fluent-predicted blade-section aerodynamic performance.

For Run 19A, the LWC was only 0.10 (Table 1), resulting in the relatively small ice shapes shown in Fig. 1(b), and Fluent predicted the R19A ice shapes to alter the 50% and 75%-station blade-section aerodynamic performance less than the ice shapes of either R3B or R21. This results in the Run 19A predicted performance change being the smallest of the three cases. The predicted reduction in C_T was predicted to be only 2% at $J = 0.78$ (Fig. 11), much smaller than the 14% C_T reduction predicted for the conditions of Run 3B (Fig. 9). The experimentally-measured reduction was much larger, nearly 9%. The smaller predicted performance reduction is likely due to the inability of the 2-D Fluent calculations to account for highly three-dimensional surface roughness on the propeller blades, resulting in unrepresentatively small blade-section performance reductions for the conditions of Run 19A. This is shown clearly in Fig. 7(c), which shows that Fluent predicted virtually no change in the 75%-station blade-section aerodynamic performance due to the Run 19A ice shape. Agreement in C_P was much better, with the predicted increase only 0.7% higher than what was measured. The predicted reduction in efficiency was only 4% (compared with a measured value of 10%), and this was largely due to the discrepancy in C_T.

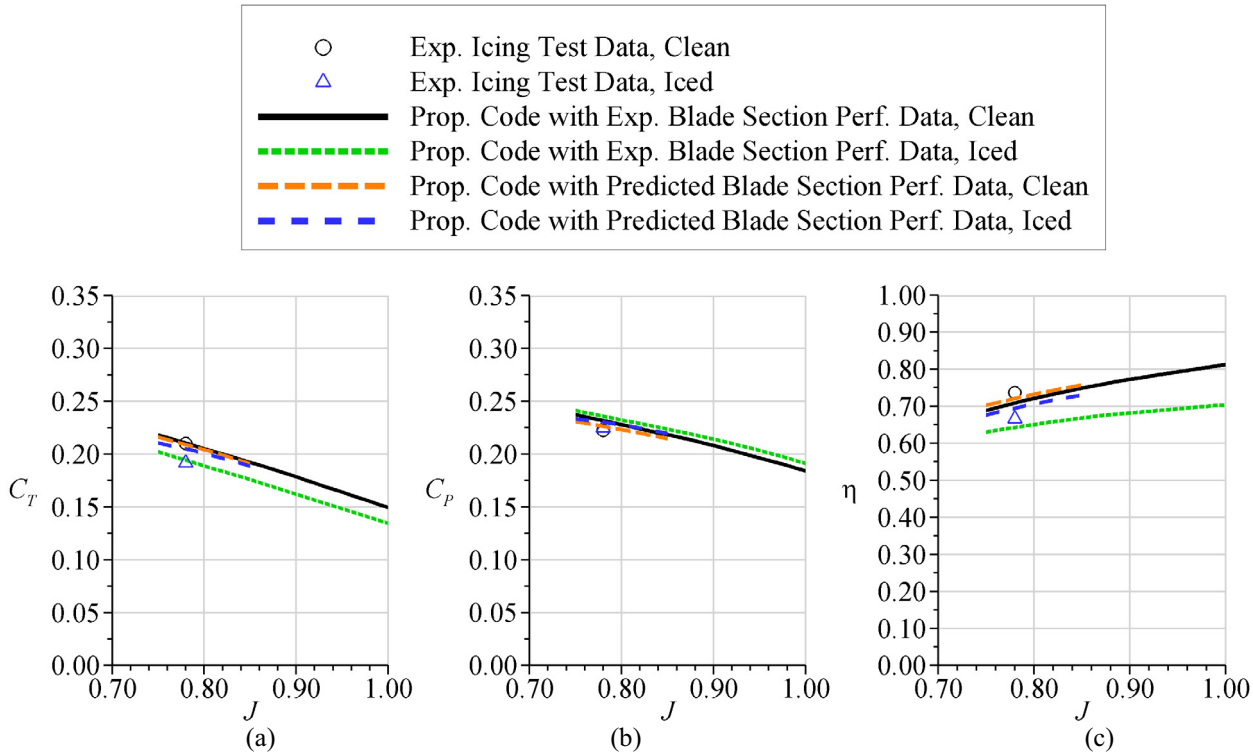

Fig. 10 Comparison of measured and predicted propeller (a) thrust coefficient, (b) power coefficient, and (c) efficiency for the icing conditions of Run 19A.

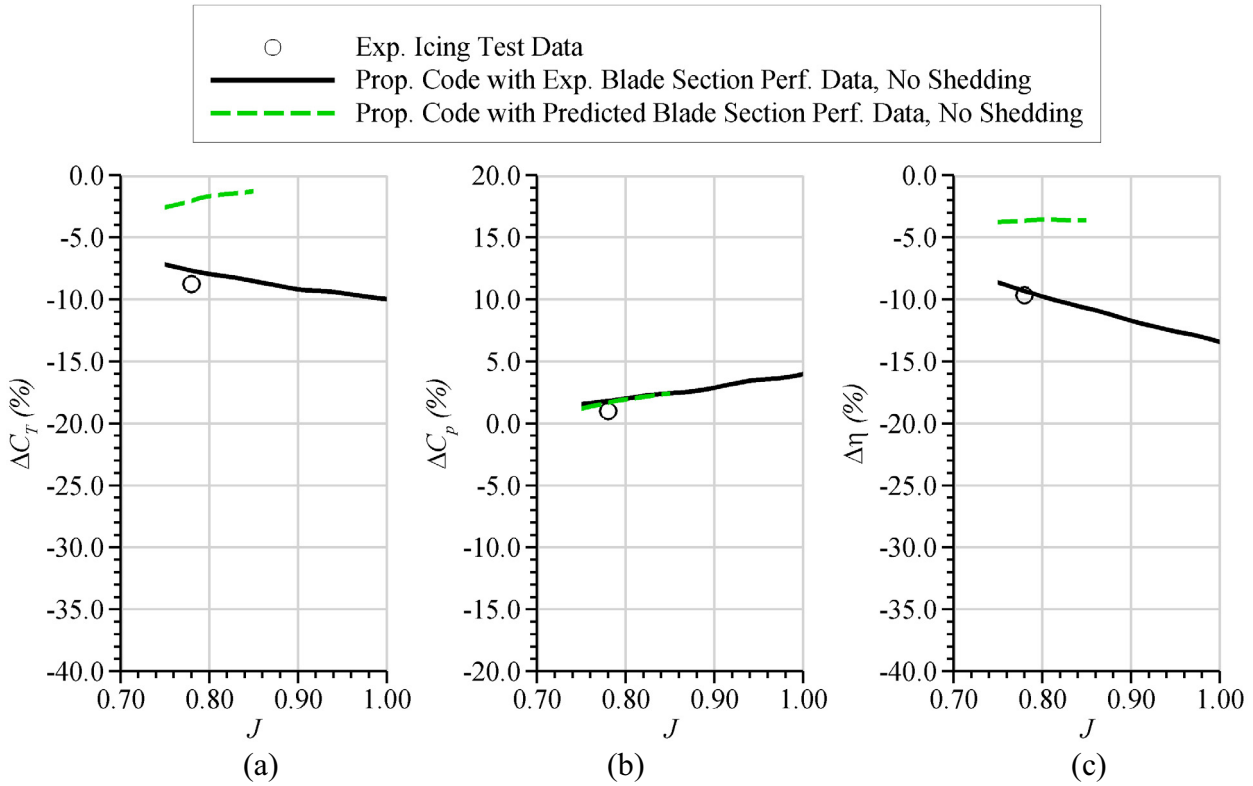

Fig. 11 Comparison of the measured and predicted change in propeller (a) thrust coefficient, (b) power coefficient, and (c) efficiency due to ice accretion from the icing conditions of Run 19A.

The results for the SLD icing conditions of Run 21 are shown in Fig. 12 and Fig. 13. Agreement between measured and predicted values of clean propeller performance is similar to the other two runs, with differences in C_T and C_p, of 3% and 4%, respectively, at $J = 0.78$. Both of these parameters were over-predicted by the code, and the error canceled out in the calculation of η, resulting in only a 1% difference between measured and predicted clean propeller efficiency. Similar, but slightly worse agreement was obtained for the iced propeller performance. The code over-predicted C_T by 8% and C_P by 1%, resulting in a 7% over-prediction of η.

The percent reduction in propeller performance due to the icing conditions of Run 21 is shown in Fig. 13. The propeller performance code with the Fluent-predicted blade section performance data under-predicted the reduction in C_T, predicting a loss of 17% compared with the experimentally-measured 21% at J= 0.78. It also under-predicted the penalty to C_p, predicting a reduction in C_P of almost 3% compared with the experimentally-measured C_P increase of 1%. These two errors combined to provide an η reduction prediction of 15%, smaller than the experimentally-measured η reduction of 22%.

The ice shapes of Run 21 were significantly larger than the shapes of Runs 3B or 19A, and ice shedding effects were found to be substantial in predicting iced propeller performance during the previous phase of this study. In that phase of the study, a series of modifications were made to the experimental iced blade-section aerodynamic performance data that was input to the blade-element code to estimate the effect that shedding could have on propeller performance. Partial ice shedding was assumed to occur at the 75% radial station based on stop-action video of the icing test at Eglin AFB. Therefore, instead of using blade-section performance data based on the 75%-station ice tracing obtained during Run 21, performance data based on the ice tracing of the much smaller Run 19A 75%-station ice shape was used to simulate the shedding. This inclusion of shedding effects had considerable effect on the predicted propeller performance (Fig. 13). At $J = 0.78$, the predicted reduction in C_T decreased from 25% to 21% when shedding was modeled (again, these predicted results use experimental blade section data obtained with artificial ice shapes as input to the blade-element propeller performance code). An even larger difference in the predicted change in C_P was observed. Without shedding, C_P was predicted to decrease by 10%; with shedding included, C_P was predicted to increase by 10%. There was a similar large variation in predicted efficiency reduction, ranging from 12% to 31%.

In the current study, the Fluent-predicted blade-section performance was modified in an identical way; the Run 19A 75%-station performance data were used instead of the Run 21 75%-station data to simulate partial shedding. However, Fig. 13 shows that the predicted effects of shedding were much smaller than when the experimental blade-section performance data were used. At $J = 0.78$, the inclusion of shedding effects caused a slightly smaller reduction in C_T of 16.5% (compared with 17.3% when shedding was ignored), and a larger reduction in C_P of 6% (compared with only 3% when shedding was ignored). The predicted efficiency drop was 12% when shedding was modeled and 15% when shedding was ignored. In Fig. 13, the relatively larger changes in predicted C_P than C_T between the cases with and without shedding were due largely to the differences in the 75%-station C_d with the Run 19A and Run 21 ice shapes (Fig. 7). Blade-section C_d affects propeller C_P more than C_T (which is mainly dependent upon blade-section C_l), explaining the larger change in predicted C_P and smaller change in C_T shown when shedding effects were considered.

The smaller difference in propeller performance degradation associated with ice shedding that was calculated using Fluent-predicted blade-section performance data is attributable primarily to a smaller difference in iced blade-section C_d at the 75% station predicted by Fluent than measured using artificial ice shapes in a wind tunnel (Fig. 7(c)). Recall that the only difference between the cases with and without shedding was the data set used for the 75%-station blade-section performance; the no-shedding case used the Run 21 aerodynamic performance data at the 75% station, and the case in which shedding was modeled used the Run 19A data. The differences in C_l between the two cases (i.e., between the iced 75%-station Run 19A shape and the iced 75%-station Run 21 shape) predicted by Fluent and measured experimentally were similar, but the differences in C_d predicted by Fluent were much smaller than the experimentally-measured differences in C_d. As discussed above, the large difference in C_d was the primary driver for the predicted performance difference between the cases with and without shedding. Since in this case the Fluent-predicted blade-section data had a much smaller difference in C_d, the predicted effects of shedding were much less significant. However, it is still recommended that a more accurate shedding model be developed and incorporated into this methodology for consideration in future cases, as it has the potential to significantly affect predicted propeller performance.

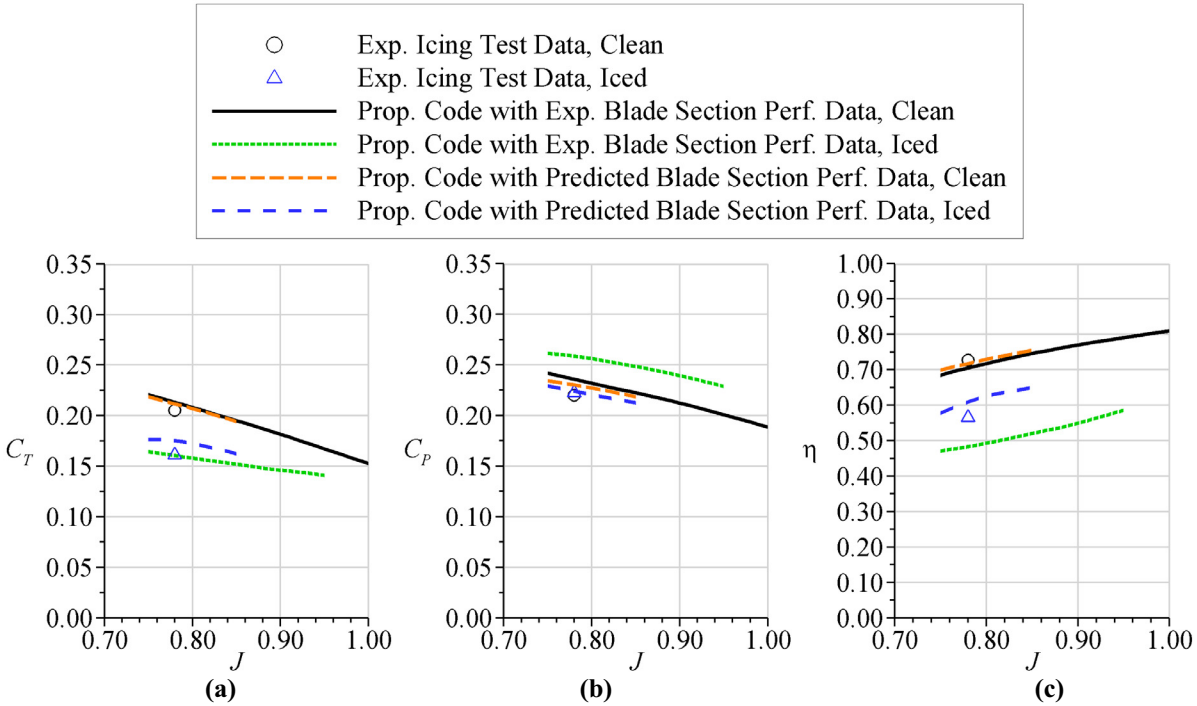

Fig. 12 Comparison of measured and predicted propeller (a) thrust coefficient, (b) power coefficient, and (c) efficiency for the icing conditions of Run 21. Ice shedding was not modeled for the data shown.

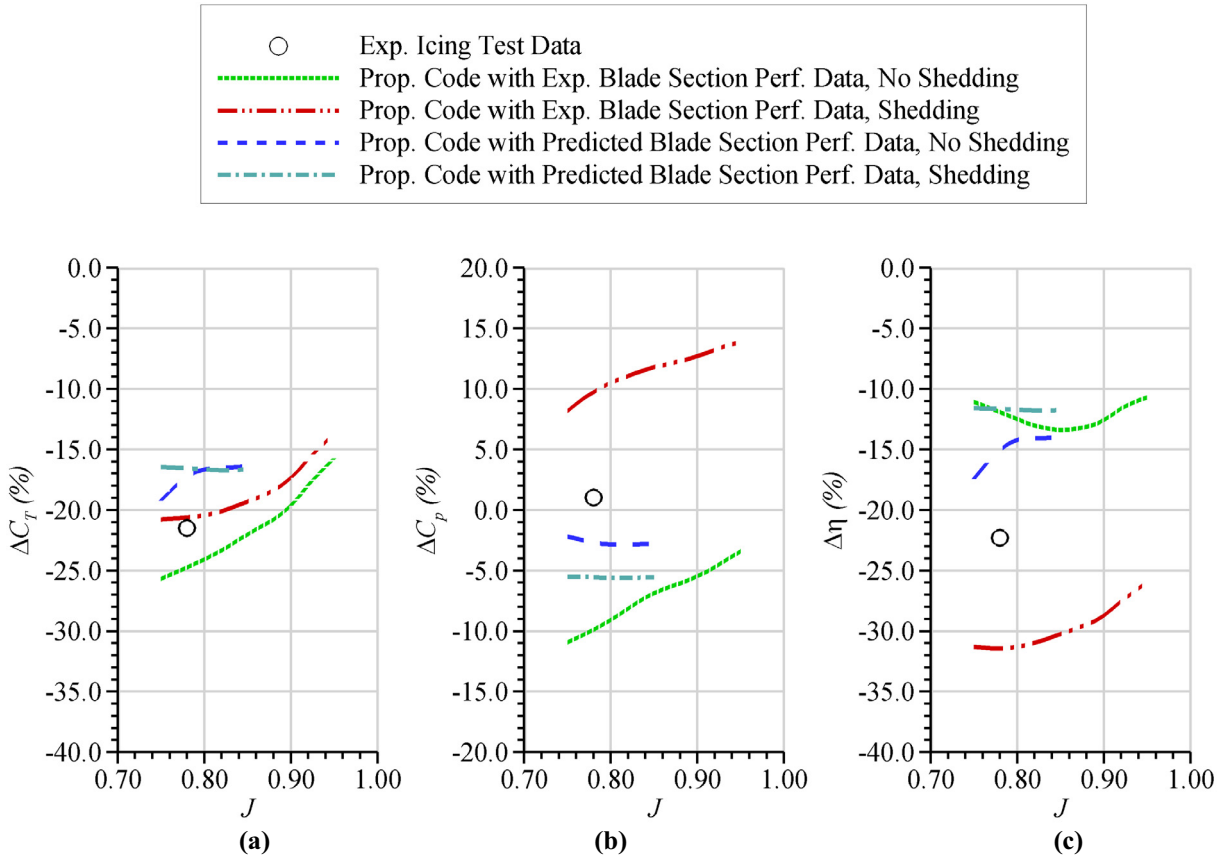

Fig. 13 Comparison of the measured and predicted change in propeller (a) thrust coefficient, (b) power coefficient, and (c) efficiency due to ice accretion from the icing conditions of Run 21.

Summary and Conclusions

The objective of the current study was to develop a computational methodology to analyze propeller performance in icing conditions and to identify areas where additional research is required. The method employed to predict iced-propeller performance in this study had three primary steps:

1) Given a propeller geometry and icing and flow conditions, use the ice-accretion prediction code LEWICE to predict the ice shapes that will form at the 25%, 50%, and 75% propeller radial stations
2) Use a 2-D RANS code, such as Fluent, to determine the blade-section aerodynamic performance degradation at each radial station due to the corresponding ice shape
3) Input the blade-section aerodynamic performance data into a blade-element code to relate the blade-section aerodynamic performance to overall propeller performance

The accuracy of this method was quantified using data from a pair of experimental tests. The first was a full-scale propeller icing test recently conducted at the McKinley Climatic Laboratory at Eglin AFB in which propeller thrust was measured and propeller ice accretion documented. This test provided ice geometry data at three radial stations for three sets of icing conditions, designated Run 3B, Run 19A, and Run 21, with which the LEWICE results could be compared, and propeller performance data with which the final propeller performance predictions of the computational methodology summarized above could be compared. In the second experimental test, artificial ice shapes, based on tracings obtained during the icing test, were used to determine the blade-section aerodynamic performance degradation due to ice at the three propeller blade stations for which ice geometry data were available: the mid-boot, 50%, and 75% stations. This second test, conducted at the University of Illinois, allowed for intermediate comparisons, as it provided blade-section performance data with which the predictions of Fluent could be directly compared.

For the propeller and icing conditions of the Eglin AFB icing test, the initial blade-section ice geometries predicted by LEWICE tended to be much larger than those measured during the icing test. This discrepancy was most likely caused by ice shedding from the propeller blades during the icing test, a phenomenon which was not initially modeled in LEWICE. Stop-action video of the icing test was reviewed to determine the approximate time and extent of shedding events, and in some cases, ice tracings were analyzed to help determine likely post-shed ice geometries. The LEWICE predictions were then revised to incorporate the most significant sheds, and agreement was much better between predicted and traced iced geometries. These results suggest that LEWICE may be able to predict blade-section ice geometries if an accurate shedding model is used. However, the shedding model used in this study was based on experimental data from the icing test, and it is recommended that additional research regarding ice shedding be conducted to develop an accurate shedding model that does not depend on such data.

Due to the large uncertainties inherent in the prediction of ice shedding on rotating propeller blades and the associated uncertainties in the LEWICE predictions, the LEWICE geometries were not used in the second phase of the study, which used Fluent to determine iced-blade section aerodynamic performance. Instead, the experimentally obtained ice tracings were analyzed in Fluent, and the results were compared with experimental blade-section data obtained during the University of Illinois wind-tunnel test described above. As was the case with the University of Illinois testing, Fluent predicted the mid-boot blade section to be the most sensitive to ice accretion and the 75%-station blade section to be the least sensitive. Qualitatively, Fluent predicted similar performance degradation as was measured experimentally for the mid-boot blade section. Quantitatively, agreement with experimental results for the mid-boot section was poor. In the clean case, this was likely attributable to the assumption of fully turbulent flow around the airfoil, and the experimental testing showed that the mid-boot section was extremely sensitive to transition location. For the iced case, the disagreement was likely due to the inability of RANS codes to accurately predict flow around a bluff-body; the mid-boot blade-section was 33% thick, and when iced likely had a highly separated, unsteady flowfield over the range of angles of attack investigated. Agreement between Fluent results and experimental data for the 50%-station blade section was considerably better. Predicted C_d was similar to measured C_d in all cases, and agreement in C_l was reasonable up until stall for all but the Run 3B case. Agreement between computational and experimental results was also much better for the 75%-station blade-section than the mid-boot. Clean blade-section C_d predicted by Fluent was in good agreement with the experimental data, although $C_{l,max}$ was about 8% low. In the iced case, agreement between clean and iced C_l was fair but it was poor for C_d, with Fluent

greatly under-predicting iced blade-section C_d at all angles of attack. This may have been partially due to the use of grit roughness on the artificial ice shapes used to generate the experimental data, whereas no additional roughness beyond that present in the tracing (which had a different "two-dimensional" character and was smoothed) was modeled in the Fluent calculations.

The Fluent blade-section aerodynamic performance data was input to the blade-element propeller code to predict clean and iced propeller performance. These data were compared with data obtained during the Eglin AFB icing test. In general, the changes in propeller C_T, C_P, and η were predicted within 8%, 4%, and 7%, respectively. For all but the iced Run 3B case, predictions of the absolute values of clean and iced C_T, C_P, and η agreed to within 10%. For the icing conditions of Run 3B, the propeller code under-predicted absolute values of iced C_T by 17%. In earlier work, ice shedding was found to have a significant impact on predicted propeller performance, potentially affecting the predicted efficiency reduction due to ice accretion by up to 19%. A shedding model incorporated into the current work, based on experimental data from the Eglin icing test, resulted in a much smaller change in predicted efficiency of only 3%. However, this result is highly dependent on the extent of shedding and exactly how it is modeled, and it is recommended that a more accurate shedding model be developed which is not dependent on experimental data.

Finally, note that the Eglin AFB icing test was conducted at a much lower freestream velocity than would be encountered in typical flight conditions (100 kts vs. 240 kts) due to facility limitations, which made the angles of attack experienced by the blade-sections higher than would be encountered in flight at most radial stations. This put portions of the propeller blade, especially near the 50%-station, into the stall regime, where the accuracy of the RANS calculations was reduced compared with angles of attack well below stall. Post-stall aerodynamic performance prediction is a known weakness of RANS methods. It is expected that at the higher freestream velocity of true flight conditions (and correspondingly lower blade-section angles of attack), better accuracy could be obtained using the computational methods described in this paper.

Acknowledgments

This work was supported by the Federal Aviation Administration (FAA) Office of Aviation Research under the grant DTFA 96-G-023. From the FAA, the authors wish to thank Jim Riley, the contracting officer's technical representative, and Chris Dumont, who provided valuable advice about the testing at McKinley, and from NASA Glenn Research Center, Andy Broeren, who offered guidance and advice throughout the course of this investigation. Thanks also go to Dominik Krug, from the Technische Universität Darmstadt, who wrote the propeller performance code while at the University of Illinois, to Austin Ellis for significant contributions with the LEWICE portion of this project while at the University of Illinois, and to Joe Bottalla at the University of Illinois for assistance in generating some of the Fluent data presented in this paper.

References

[1] Timmons, L., "Icing Investigations and Product Development on MU-2B Airplanes," SAE 2003-01-2088, FAA In-Flight Icing/Ground De-icing International Conference, Chicago, IL, Jun. 2003.

[2] Dumont, C., Pellicano, P., Smith, T., and Riley, J., "Results From a Full-Scale Propeller Icing Test," AIAA Paper 2008-0432, *46th AIAA Aerospace Sciences Meeting & Exhibit*, Reno, NV, Jan. 2008.

[3] Busch, G., Bragg, M., and Brroeren, A., "Prediction of Propeller Performance in Icing Conditions Using Vortex Theory," AIAA-2009-4259, *1st AIAA Atmospheric and Space Environments Conference*, San Antonio, TX, Jun. 2009.

[4] Corson, Jr., B.W., and Maynard, J.D., "The Effect of Simulated Icing on Propeller Peformance," NACA TN-1084, Jul. 1946.

[5] Preston, G.M., and Blackman, C.C., "Effects of Ice Formations on Airplane Performance," NACA TN-1598, May 1948.

[6] Neel, Jr., C.B., and Bright, L.G., "The Effect of Ice Formations on Propeller Performance," NACA TN-2212, Oct. 1950.

[7] Korkan, K.D., Dadone, L., Shaw, R.J., "Performance Degradation of a Propeller System Due to Rime Ice Accretion," *J. Aircraft*, v. 21, n. 1, 1984, pp. 44-49.

[8] Miller, T.L., Korkan, K.D., and Shaw, R.J., "Analytical Determination of Propeller Performance Degradation due to Ice Accretion," *J. Aircraft*, v. 24, n. 11, 1987, pp. 768-775.

[9] Bragg, M.B., "Rime Ice Accretion and Its Effect on Airfoil Performance," NASA CR 165599, Mar. 1982.
[10] Gray, V.H., "Prediction of Aerodynamic Penalties Caused by Ice Formations on Various Airfoils," NASA TN-D 2166, Feb. 1964.
[11] Flemming, R.J., and Lednicer, D.A., "High Speed Ice Accretion on Rotorcraft Airfoils," NASA CR 3910, Aug. 1985.
[12] Reichhold, J., Bragg, M., and Sweet, D., "Experimental Determination of the Droplet Impingement Characteristics of a Propeller," AIAA Paper 97-0179, *35th AIAA Aerospace Sciences Meeting & Exhibit*, Reno, NV, Jan. 1997.
[13] Farag, K.A., and Bragg, M.B., "Three Dimensional Droplet Trajectory Code for Propellers of Arbitrary Geometry," AIAA Paper 98-0197, *36th AIAA Aerospace Sciences Meeting & Exhibit*, Reno, NV, Jan. 1998.
[14] Bragg, M., Broeren, A., Addy, H., Potapczuk, M., Guffond, D., and Montreuil, E., "Airfoil Ice Accretion Aerodynamic Simulation," AIA-2007-0085, *45th AIAA Aerospace Sciences Meeting & Exhibit*, Reno, NV, Jan. 2007.
[15] Busch, G., "Experimental Study of Full-Scale Iced-Airfoil Aerodynamic Performance Using Sub-Scale Simulations," Ph.D Dissertation, University of Illinois at Urbana-Champaign, 2009.
[16] Wright, W., "Validation Results for LEWICE 3.0," AIAA-2005-1243, *43rd AIAA Aerospace Sciences Meeting & Exhibit*, Reno, NV, Jan. 2005
[17] http://my.fit.edu/itresources/manuals/fluent6.3/help/html/ug/main_pre.htm
[18] Spalart, P.R. and Allmaras, S.R., "A One-Equation Turbulence Model for Aerodynamic Flows," AIAA-1992-0439, *30th AIAA Aerospace Sciences Meeting &* Exhibit, Reno, NV, Jan. 1992.
[19] Chung, J.J., and Addy, Jr., H.E., "A Numerical Evaluation of Icing Effects on a Natural Laminar Flow Airfoil," AIAA-2000-0096, *38th AIAA Aerospace Sciences Meeting & Exhibit*, Reno, NV, Jan. 2000.
[20] Chi, X., Zhu, B., Shih, T.I.P., Add, H.E., and Choo, Y.K., "CFD Analysis of the Aerodynamics of a Business-Jet Airfoil with Leading-Edge Ice Accreteion," AIAA-2004-0560, *42nd AIAA Aerospace Sciences Meeting and Exhibit,* Reno, NV, Jan. 2004.
[21] White, F.M. *Viscous Fluid Flow*, 3rd Ed., McGraw-Hill, 2005.
[22] Jacobs, J., "Iced Airfoil Separation Bubble Measurements by Particle Image Velocimetry," Ph.D Dissertation, University of Illinois at Urbana-Champaign, 2007.
[23] http://202.118.250.111:8080/fluent/Gambit13_help/users_guide/ugtoc.htm
[24] http://jullio.pe.kr/fluent6.1/help/html/ug/node455.htm#sec-guidelines-twolayer
[25] Vickerman, M.B., Choo, Y.K., Schilling, H.W., Baez, M., Braun, D.C., and Cotton, B.J., "Toward an Efficient Icing CFD Process Using an Interactive Software Toolkit – SmaggIce 2D," AIAA-2002-0380*, 40th AIAA Aerospace Sciences Meeting & Exhibit*, Reno, NV, Jan. 2002.
[26] Chung, J., Reehorst, A.L., Choo, Y.K.,and Potapczuk, M.G., "Effect of Airfoil Ice Shape Smoothing on the Aerodynamic Performance," AIAA-1998-3242, *34th AIAA/ASME/SAE/ASEE Joint Propulsion Conference and Exhibit*, Cleveland, OH, Jul. 1998.
[27] McCormick, B.W., *Aerodynamics, Aeronautics, and Flight Mechanics*, 2nd Ed., John Wiley & Sons, 1995.
[28] Krug, D., "Development of a Propeller Performance Code," Independent Study Rept., Technische Universität Darmstadt and University of Illinois, Jun. 2008.
[29] Van Rooij, R.P.J.O.M. and Timmer, W.A., "Roughness Sensitivity Considerations for Thick Rotor Blade Airfoils," *Journal of Solar Energy Engineering*, Vol. 125, Issue 4, Nov. 2003, pp. 468 – 478.
[30] Kim, H.S., and Bragg, M.B., "Effects of Leading-edge Ice Accretion Geometry on Airfoil Aerodynamics," AIAA-1999-3150, *17th AIAA Applied Aerodynamics Conference*, Norfolk, VA, Jun. 1999.